Dynamic Deformation Under a Modified Split Hopkinson Pressure Bar Experiment

Ouk Sub Lee*, Seung Suk You, Ju Ho Chong** and Hee Soo Kang****

(Received March 26, 1998)

This paper presents a modified split-Hopkinson pressure bar (SHPB) technique. The dynamic stress-strain behaviors were estimated at room temperature and subzero temperature to -75℃ by using the conventional SHPB and compared with a modified SHPB technique. A computer simulation using a finite element algorithm is also performed to study the dynamic material responses. Furthermore, we attempt to find a proper material constitutive law by using the simulation process. It is suggested that the modified SHPB test used in this study can be successfully utilized to offer an experimental condition of a higher strain rate than that obtained from the conventional SHPB test.

Key Words: Computer Simulation, Dynamic Deformation, High Strain Rate, Modified Split Hopkinson Pressure Bar

1. Introduction

The stress-strain responses and dynamic fracture characteristics of various engineering materials under dynamic loading conditions have been determined mainly using the Split Hopkinson Pressure Bar (SHPB) technique and instrumented Charpy impact test by many researchers (Lee, 1997, Meyers, 1994, Meyer, 1992, Zukas, 1990). The SHPB technique has been popularly used for strain rates ranging from 10^2 to 10^4/s. To enhance the strain rate up to 10^7/s, various types of accelerators, such as electrostatic, electromagnetic, explosive and plasma accelerators, light-gas guns or pulsed lasers have been used in conjunction with the high velocity impact SHPB technique.

This paper presents a simple way to achieve the high strain rate loading condition. A modified SHPB technique is described in order to determine the dynamic stress-strain behavior. This paper also presents experimental results for Al 2024-T3 (which is known as a ductile aluminum alloy at room temperature under the static loading condition) obtained from both the conventional and the modified SHPB techniques under compressive loadings at low temperatures to -75℃. Constitutive equations fit to the dynamic stress-strain response are also discussed.

* Department of Mechanical Engineering, Inha Univ., Inchon 402-751, Korea

2. Basic Principle

2.1 The conventional SHPB test

The principle relevant equations for the SHPB technique are well documented (Meyers, 1994, Zukas, 1990, Dharan and Hauser, 1970). A brief summary is given below. A small specimen is positioned between two long bars made of a high strength material. The bars remain elastic while the specimen deforms plastically under a striker impact loading. Figure 1 shows a schematic diagram of the specimen and elastic stress waves for the compressive SHPB test.

When the incident bar is impacted by the striker bar, rectangular stress pulse is generated and travels along the incident bar until it hits the specimen. Part of the incident stress pulse is reflected from the specimen because of the material impedance mismatch between the specimen and incident bar, and part of it transmits through the specimen. Within the specimen positioned between the incident and transmitted bars, the

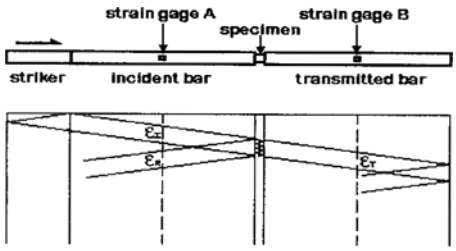

ε_I : *incident strain*, ε_R : *reflected strain*, ε_T : *transmitted strain*

Fig. 1 A schematic diagram of specimen and elastic stress waves for the SHPB test (the subscripts I, R, and T refer to the incident, reflected and transmitted pulses, respectively).

stress pulses are reflected back and forth at both ends of the specimen to reach an equilibrium state. The transmitted pulse emitted from the specimen travels along the transmitted bar until it hits the end of the bar.

The incident and transmitted bars are long enough to minimize the effect of reflected stress waves from the end of the bars on the strain gage positioned on the bars. The stress pulse is assumed to be a nondispersive elastic wave and the specimen is usually short so that the equilibrium state can be reached after many stress wave reflections take place within the specimen. The stress and strain in the specimen can be obtained in terms of the recorded strains of the two bars as

$$\sigma_{specimen}=E\left(\frac{A}{A_s}\right)\varepsilon_T \tag{1}$$

$$\varepsilon_{specimen}=\left(\frac{-2C_0}{L}\right)\int_0^t \varepsilon_R dt \tag{2}$$

where E, A, and C_0 are the elastic modulus, the cross-sectional area and the longitudinal wave speed of the bars, respectively. L and As are the length and the cross-sectional area of the specimen, respectively.

2.2 A modified SHPB test

The technique modified by Hauser (Dharan and Hauser, 1970) was utilized to measure the material response under the strain rate higher than that obtained by using the conventional SHPB technique. A loading device was constructed to achieve the high stresses necessary. Figure 2 shows an experimental arrangement for the

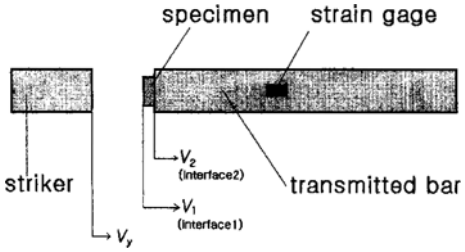

Fig. 2 A schematic experimental arrangement for a modified SHPB technique.

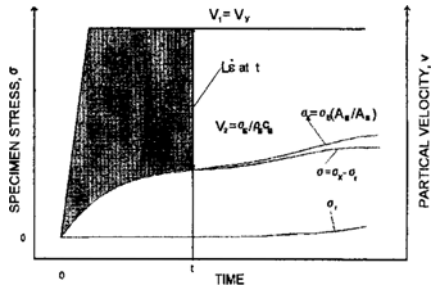

Fig. 3 Fundamental concept for determination of the stress, strain and strain rate from the strain-gage output and the striker velocity.

modified SHPB experiment, where V_1 and V_2 are the particle velocities in the specimen ends, respectively.

A limitation of the conventional SHPB technique is that the striker impact velocity is restricted to keep the input bar material within the elastic range. The striker impact velocities are, thus, limited to velocities less than

$$V_y=\frac{\sigma_y}{\rho C} \tag{3}$$

where V_y is the limiting striker impact velocity. σ_y, ρ, and C are the elastic limit, the mass density and the longitudinal wave velocity in the incident bar, respectively.

V_y for the material used in the conventional SHPB test is 80m/s. To allow the higher striker impact velocities, the incident bar was removed and the striker impact bar was permitted to hit the specimen directly. The transmitted bar backs up the specimen as in the conventional SHPB technique. Figure 3 shows the basic concept for determination of the stress, strain and strain rate from the strain gage output in the transmitted bar.

The particle velocity in the specimen at inter-

face 1 was assumed to be the same as that of the striker velocity with a finite rise time. The stress transmitted by the specimen travels along the transmitted elastic output bar. The magnitude of the dynamic strain was monitored by the strain gages on the bar. The dynamic stress was determined by using Hooke's law as $\sigma_E = \varepsilon_E E$. The particle velocity, V_2, in the specimen at interface 2 can be obtained as

$$V_2 = \frac{\sigma_E}{\rho_E \cdot C_E} \tag{4}$$

where the subscript E refers to the elastic transmitted bar. Then, the average strain rate in the specimen at any time during dynamic deformation can be estimated as

$$\dot{\varepsilon} = \frac{V_1 - V_2}{L} \tag{5}$$

where L is the gage length of the specimen. The average strain of the specimen can be given by

$$\varepsilon = \int_0^t \frac{V_1 - V_2}{L} \tag{6}$$

The average stress at any time in the specimen corrected by reflecting the radial stresses due to the radial and tangential particle velocities is given by

$$\sigma = \sigma_x - \sigma_r \tag{7}$$

where

$$\sigma_x = \frac{A_E}{A_S}\sigma_E,\ \sigma_r = \frac{3}{8}\rho\left(\frac{a_0}{l_0}\right)^2 \frac{v_x^2}{(1-\varepsilon_x)^3}$$

A_E and As indicate the cross-sectional area of the elastic transmitted bar and the specimen, respectively ρ, a_0 and l_0 are the density of the specimen material, the initial dimensions of the radius and the length of the specimen. v_x is the constant axial velocity and ε_x can be determined from the experimental data. Eqs. (6) and (7) are solvable following the procedure appeared in Figure 3 using stress-time relationship measured by the strain gages on the elastic transmitted bar.

3. Experimental Results

Figure 4 shows the general experimental setup and various striker bars, specimen geometry

(a) A general view of SHPB experiment setup.

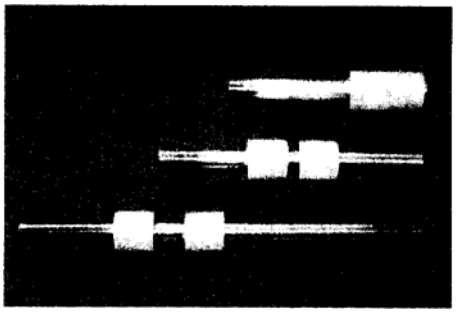

(b) Various striker bars.

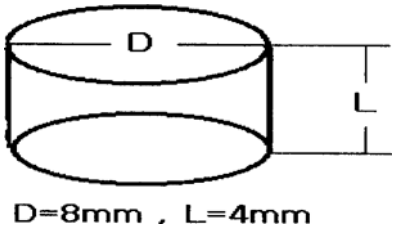

(c) Specimen geometry.

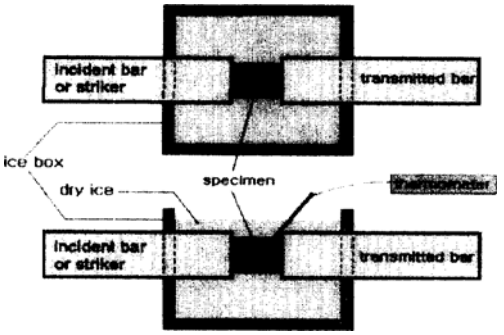

(d) Subzero temperature test setup.

Fig. 4 General views and schemetic diagrams of various SHPB experimental equipments.

and a setup for the subzero temperature experiment used for the conventional and a modified SHPB techniques. Minimizing the inertia effect to radial direction appeared in Eq. (7), we chose the ratio of the diameter to length of the specimen as 2 : 1 to meet the condition of Eq. (8) (Davies and Hunter, 1963).

$$\frac{L}{D}=\sqrt{\frac{3\nu_s}{4}} \tag{8}$$

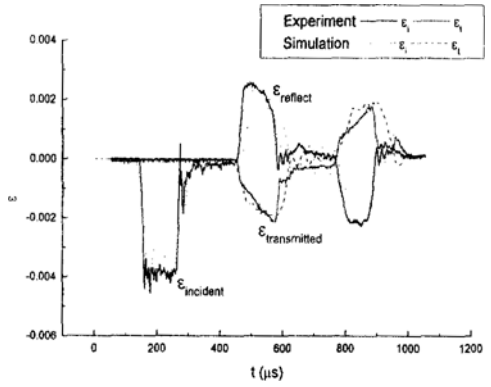

(a) Conventional SHPB.

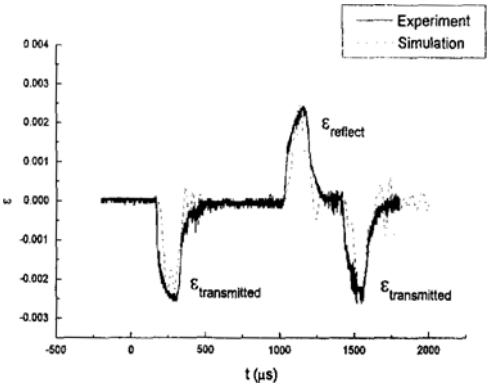

(b) Modified SHPB.

Fig. 5 Typical strain output and a computer simulation for two results.

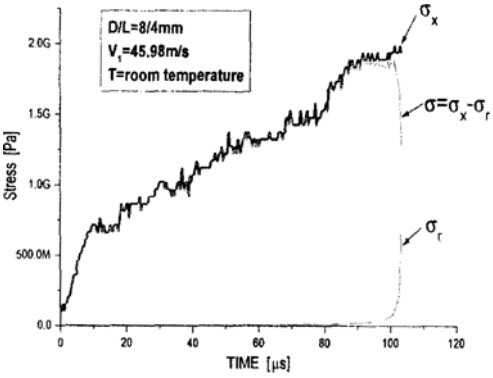

Fig. 6 Experimental stresses (σ_x) with calibration stresses (σ_r)

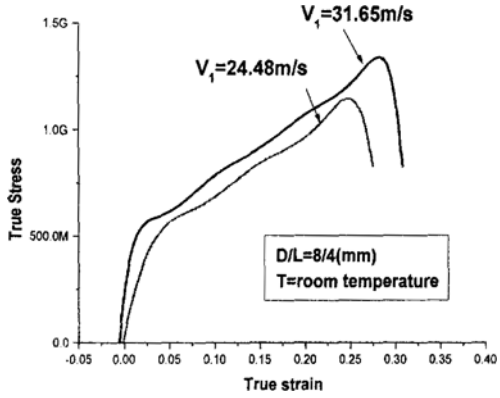

Fig. 7 Stress-strain relationships of Al 2024-T3 at different striker velocities by using the conventional SHPB.

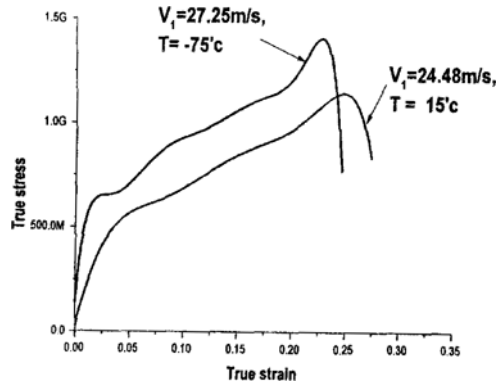

Fig. 8 Stress-strain relationships of Al 2024-T3 at different temperatures by using the conventional SHPB.

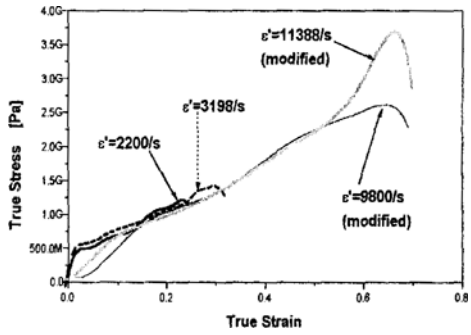

Fig. 9 Stress-strain behavior at various strain rates.

where v_s is the poisson ratio of the specimen.

Figure 5 shows the typical strain output obtained by the conventional and the modified SHPB techniques. Solutions obtained by a computer simulation (dotted in the figure) are found to agree well with the experimental results.

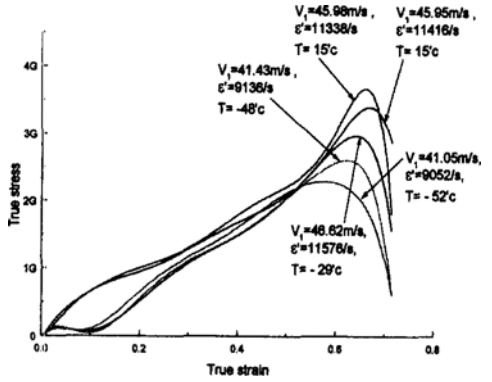

Fig. 10 Stress-strain relationships of Al 2024-T3 at different temperatures and striker velocities by using a modified SHPB.

Figure 6 shows experimental stresses with calibration stresses by using Eq. (7).

Figures 7 and 8 show the stress-strain relationships at different striker velocities and different temperatures by using the conventional SHPB.

Figure 9 shows stress-strain behaviors at various strain rates by using the conventional SHPB and a modified SHPB techniques.

Figure 10 shows the stress-strain relationships at different striker velocities and different temperatures by using the modified SHPB. It is interesting to note that the effect of strain rate is more pronounced than that of temperature. We may need to do in-depth investigation on this curious findings.

The stress-strain behaviors at room and subzer-

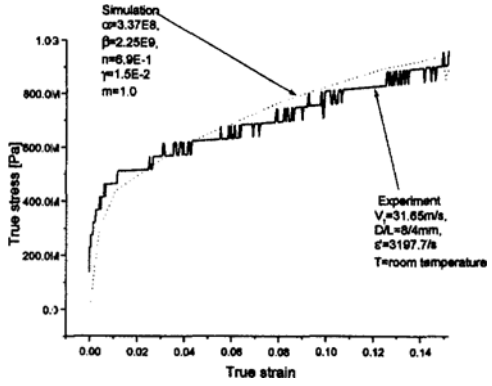

(a) Conventional SHPB at room temperature.

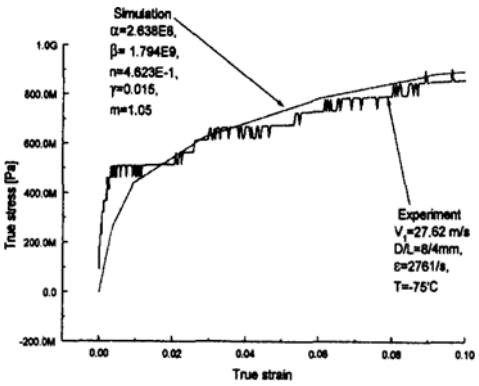

(b) Conventional SHPB at -75℃. (continued)

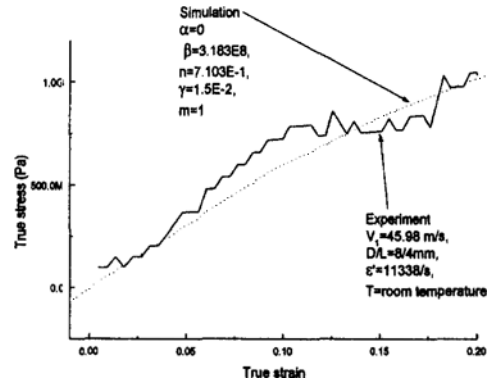

(c) Modified SHPB at room temperature. (continued)

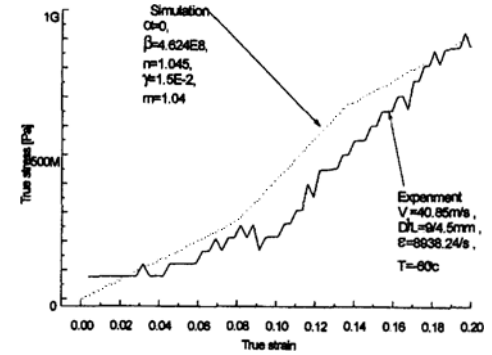

(d) Modified SHPB at -60℃. (continued)

Fig. 11 Dynamic stress-strain behaviors for Al 2024-T3 obtained from two SHPB techniques and a computer simulation

o temperatures for Al 2024-T3 specimens estimated by two techniques are shown in Fig 11. A computer simulation using the Johnson-Cook constitutive model such as Eq. (9) (Meyers, 1994 and Zukas, 1990) is also included in Fig. 11.

$$\sigma=[\alpha+\beta(\bar{\varepsilon}^{p})^{n}][1+\gamma\ln\dot{\varepsilon}^{*}][1-(T^{*})^{m}] \quad (9)$$

where α is the yield stress constant, β is the strain hardening coefficient, n is the strain hardening exponent, γ is the strain rate dependent coefficient and m is the temperature dependence exponent. Johnson-Cook provided constants such as α, β, γ, n and m, for 6 ductile and 6 less ductile materials, including Cu, Fe, brass, Ni, C-steel, tool steel, Al alloys, and DU. By this broad source of data, the Johnson-Cook equations are often used as constitutive equations for the numerical analysis like FEM (Meyer, 1992). $\dot{\varepsilon}^{*}(=\dot{\varepsilon}/\varepsilon_0$, where ε_0=standard equivalent plastic strain rate) can be obtained by the experiment, and the homologuous temperature T^{*} is the ratio of the current temperature to the melting temperature, where $T^{*}=(T-T_r)/(T_m-T_r)$, T_r is the room temperature and T_m is the melting temperature.

All the unknown parameters were determined by using nonlinear least square best fitting procedures.

The agreement between the experimental results and numerical simulations is found to be reasonably good up to the strain of about 0.2 .

The strain rates estimated by using a the modified SHPB test with the same striker velocities are approximately 5 times higher than those obtained from the conventional SHPB test.

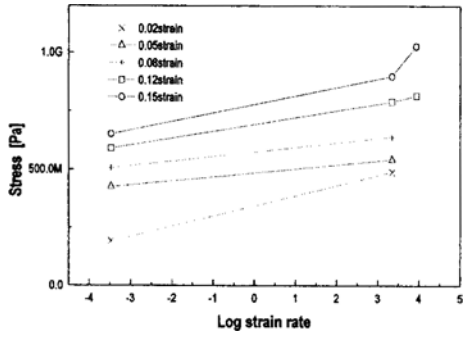

Fig. 12 Relationship between strain rates and yield stresses for Al 2024-T3.

Furthermore, we could obtain the stress-strain data up to a very high deformation state of a strain about 0.7 by using the modified SHPB test as shown in Fig. 10. The variations of the yield stress in accordance with the strain rate for Al 2024-T3 are given in Fig 12. A typical linear relationship is noted between the strain rate and yield stresses on a semi-log scale .

4. Conclusions

Under the similar experimental condition, the higher strain rate deformation, 5 times higher than those by using the conventional SHPB test, was obtained with the help of a modified SHPB test procedure for Al 2024-T3 which behaves as a ductile material at room temperature under static loading conditions. The deviation of the yield stresses from the linear relationship between the logarithmic strain rate and the yield stresses is pronounced at a strain rate of around 10^4/s as appeared in many published studies. It seems that the necessary experimental conditions for the quasi-equilibrium state are obtained in the specimen during the modified SHPB test procedure.

The effect of low temperature to -75℃ on the dynamic stress-strain relationship is found to be negligible under strain rate of $2.7\sim3.1\times10^3$/s loading condition.

Acknowledgment

The authors appreciate the financial supports from the ADD (ADD-TEMD-413-971480) during this investigation.

References

Davies, E. D. H. & Hunter, S. C., 1963, "The Dynamic Compression Testing of Solids by the Method of the Split Hopkinson Pressure Bar," *J. Mech. Phys. Solids,* Vol 11, p. 155

Dharan, C. K. H. & Hauser, F. E., 1970, "Determination of Stress-Strain Characteristics at Very High Strain Rates," *Experimental Mechanics,* Sep. pp. 370~376.

Kolsky, H., 1963, "Stress Waves in Solids. New

York Dover Publications," Inc.

Lee, O. S. & Hong, S. K., 1997, "Dynamic Fracture Characteristics of Highly Brittle Materials by Using Instrumented Charpy Impact Test," *KSME International Journal,* Vol. 11, No. 5, pp. 513~520

Meyers, M. A., 1994, "Dynamic Behavior of Materials," Wiley & Sons, Inc.

Meyers, M. A., Murr, L. E. & Straudhammer, K. P., 1992, (eds.) "Shock-Wave and High Strain -Rate Phenomena in Materials," Marcel Dekker, Inc., pp. 49~59

Murr, L. E., Meyers, M. A. & Straudhammer, K. P., 1995, (eds.) "Metallurgical and Materials Applications of Shock-Wave and High Strain Rate Phenomena."

Zukas, J. A., 1990., (eds.). "High Velocity Impact Dynamics," John Wiley & Sons, Inc.